Heliyon 10 (2024) e27421

Contents lists available at ScienceDirect

Heliyon

journal homepage: www.cell.com/heliyon

Review article

Development and advancements in rodent MRI-based brain atlases

Xiaoyi Ma [a,1], Yao Xing [b,c,1], Renkuan Zhai [c], Yingying Du [c], Huanhuan Yan [d,e,*]

[a] Department of Geriatrics, The First Affiliated Hospital, Sun Yat-Sen University, Guangzhou, 510080, China
[b] School of Information Science and Technology, Fudan University, Shanghai, 200433, China
[c] Wuhan United Imaging Life Science Instrument Co., Ltd., Wuhan, 430071, China
[d] Shenzhen United Imaging Research Institute of Innovative Medical Equipment, Shenzhen, 518048, China
[e] Paul C. Lauterbur Research Center for Biomedical Imaging, Shenzhen Institutes of Advanced Technology, Chinese Academy of Sciences, Shenzhen, 518055, China

ARTICLE INFO

Keywords:
Brain atlases
Rodent
Magnetic resonance imaging
Neuroscience
Brain structures

ABSTRACT

Rodents, particularly mice and rats, are extensively utilized in fundamental neuroscience research. Brain atlases have played a pivotal role in this field, evolving from traditional printed histology atlases to digital atlases incorporating diverse imaging datasets. Magnetic resonance imaging (MRI)-based brain atlases, also known as brain maps, have been employed in specific studies. However, the existence of numerous versions of MRI-based brain atlases has impeded their standardized application and widespread use, despite the consensus within the academic community regarding their significance in mice and rats. Furthermore, there is a dearth of comprehensive and systematic reviews on MRI-based brain atlases for rodents. This review aims to bridge this gap by providing a comprehensive overview of the advancements in MRI-based brain atlases for rodents, with a specific focus on mice and rats. It seeks to explore the advantages and disadvantages of histologically printed brain atlases in comparison to MRI brain atlases, delineate the standardized methods for creating MRI brain atlases, and summarize their primary applications in neuroscience research. Additionally, this review aims to assist researchers in selecting appropriate versions of MRI brain atlases for their studies or refining existing MRI brain atlas resources, thereby facilitating the development and widespread adoption of standardized MRI-based brain atlases in rodents.

1. Introduction

Mice and rats are extensively utilized in neuroscience research. As the size and complexity of neuroscience datasets continue to expand, the availability of publicly accessible brain atlases becomes increasingly indispensable. Brain atlases facilitate the precise localization of diverse data types within a unified 3D space, enabling their comparison, correlation, and analysis. Furthermore, they serve as versatile tools in the field of neuroscience, fulfilling various purposes such as neuroanatomy teaching, providing standardized nomenclature for brain regions, aiding researchers in data localization, and consolidating existing knowledge on brain structure and function for the academic community as a whole [1,2].

Traditional brain maps are mainly printed books based on histological section information, which include detailed textual

* Corresponding author. Shenzhen United Imaging Research Institute of Innovative Medical Equipment, Shenzhen, 518048, China.
E-mail address: hh.yan@siat.ac.cn (H. Yan).
[1] These authors contributed equally to this work.

https://doi.org/10.1016/j.heliyon.2024.e27421
Received 25 January 2023; Received in revised form 15 February 2024; Accepted 28 February 2024
Available online 8 March 2024

explanations, representative histological pictures, and drawn line drawings in three directions (coronal, sagittal, transverse) [3–8], such as the famous Paxinos and Franklin's mouse brain atlas (PF) [3], Paxinos and Watson's rat brain atlas [8]. The initial iteration of the digital brain atlas in computer graphics was the inaugural edition of "Brain Maps: Structure of the Rat Brain," which was first published in 1992 [9,10]. Since then, this atlas has undergone multiple revisions and is currently in its fourth edition [11]. In addition, the first whole-brain-scale mesoscale mouse brain atlas (Allen Mouse Brain Connectivity Atlas) was born based on serial two-photon tomography and automated vibrating microtome, which led to the birth of the famous Allen Mouse Brain Common Coordinate Framework [12,13]. These brain atlases find extensive utilization among neuroscientists worldwide and represent the most widely cited category of research within the neuroscience domain.

Despite their historical significance as essential tools in neuroscience, traditional brain atlases have several limitations. First, early histological atlases were usually generated from one or a few samples [14–16], resulting in the information presented by such brain atlases being biased towards individual brain anatomy and not representative of the population. It is well known that different strains of rodents have differences in brain morphology, and there may also be differences between rodents of the same strain from different laboratories. Second, the size and shape of the brain may alter as a result of postmortem changes brought on by anatomical and histological preparations made during sample preparation. Tissue may be altered by shrinking, stretching, and ripping as a result of histological processing procedures such fixation, embedding, sectioning, and staining [17]. As young animal brain tissue is particularly delicate and readily distorted in comparison to adult mouse/rat brain, this shift may be more pronounced in embryonic or neonatal mouse/rat brain samples [18,19]. Third, owing to the tremendous amount of time and work required for data gathering, slices are often shown at intervals of hundreds of micrometers (or even millimeters in certain situations) [20–22]. Fourth, anatomical boundaries often vary by a few millimeters in unforeseen directions across sections as a result of discrepancies between planar sections, such as various retraction errors [23]. Fifth, the inability of two-dimensional atlases to visualize brain regions in three dimensions (3D) is one of their fundamental limitations. Converting annotated 2D structures under coronal view into 3D volumes in non-coronal planes causes image distortions [12]. Lastly, traditional brain maps lack the cellular-level resolution necessary for transcriptomic studies focused on brain neurons [12].

We need constantly update brain atlases to keep up with the times, but these traditional brain atlases can no longer accommodate these three-dimensional datasets with cellular-level resolution. Compared with two-dimensional maps, digital three-dimensional maps are more in line with current research needs. For example: in the past decade, with the establishment of the mouse whole brain mapping project, new data types have been added, and rich details of the cellular structure have been continuously revealed, resulting in the most detailed 3D mouse brain atlas to date: The third edition of the Allen Mouse Brain Common Coordinate Framework (CCFv3) [13]. After arranging/integrating various types of datasets into CCFv3 format, the researchers were able to label up to 800 brain structures, identifying several brain structures that were not previously presented in the standard mouse whole-brain atlas and newly discovered several nerve fiber bundles that had never been reported in other atlases [13]. Moreover, the Unified mouse atlas from the KIM lab unified inconsistencies in the anatomical division and nomenclature of the PF and CCFv3 atlases [24]. However, also as an essential model animal in neuroscience research, the development of the rat brain atlas based on histological sections has significantly lagged behind the development of the mouse brain atlas. The possible reason is that the rat brain tissue is significantly larger than the mouse brain tissue, which increases the difficulty of developing the former.

With the application of in vivo brain imaging technology in rodent models, magnetic resonance imaging (MRI) has emerged as a crucial technique for creating rodent brain maps during the past two decades. MRI was originally (and is wide) used for non-invasive imaging of the human brain. With increased magnetic field strength and improved coil design, it now allows imaging of rodents with micron-level resolution [25]. Although the resolution and tissue specificity of MRI images are not comparable to those of histology, the development of MRI-based atlases of the animal brain still has multiple advantages. First, because MRI is non-invasive imaging, MRI-based brain atlases have higher anatomical fidelity [26]. Second, digital MRI brain atlases enable for flexible exploration of brain slices and may be constantly updated as new information becomes available [27–29]. Third, isotropic datasets may be resliced to any plane, whereas MRI brain maps are fundamentally 3D data. Without using laborious 3D reconstruction techniques, they may be processed and evaluated in any desired oblique orientation [30]. Fourth, we can often obtain MRI images from live animals, so the imaging process minimally disturbs the anatomical information presented in these images [26]. This characteristic enables population stereotaxic brain templates to be created and allows for the objective quantitative examination of anatomical diversity in the brain [31]. Fifth, compared to mice, MRI is especially suitable for brain atlas development in rats [32]. Sixth, it can make certain brain phenotypes more easily analyzeable by high-throughput computers [33,34].

Advances in technology have gradually narrowed the shortcomings of MRI brain atlases compared to histological brain atlases. In terms of resolution, resolutions of 21.5 μm and 50 μm can now be routinely achieved in MR images of ex vivo and in vivo mouse brains, respectively [18,25]. While this is still not comparable to the highest resolutions achievable by a light microscope, it has been at the level of a low-magnification microscope. The brain tissue image contrast achievable by MRI has also improved with the application of various MRI pulse sequences (such as T1, T2, T2*, diffusion, and magnetization transfer) and contrast agents (such as Gd^{3+}, Mn^{2+}, Cu^{2+}, Fe^{3+}, and Cr^{6+}) [26]. These MR images' contrast reflects the physical and chemical milieu of water molecules found in tissue, including the presence of myelin and water [35]. While histology provides more sensitivity and specificity than MRI contrast, MRI is a better imaging tool for many research due to its ability to track anatomical and physiological changes in the body. Furthermore, MRI brain atlases are essential for such studies.

In light of the advantages offered by MRI technology and the progress made in ultra-high-field small animal MRI equipment, scientists have developed various iterations of mouse and rat MRI brain atlases. A comprehensive review of MRI brain atlases for mice and rats is presented in Tables 1 and 2, respectively. Furthermore, Fig. 1A and B illustrate a selection of commonly used mouse and rat brain atlas exemplars, respectively. These atlases typically involve delineation of specific anatomical components and encompass a

Table 1
Overview of mouse MRI brain atlas research (in reverse order of publication time and version).

Name	Strains	Number of mice	Age	In vivo/ Ex vivo	Field	Contrast	Spatial Resolution (mm^3)	Scan duration	Template	Atlas	Brain structures	GM, WM, CSF priors	Link	Reference (s)
Ren_2021	BALB/c	4 males and 9 females	14 m	In vivo	7T	T2	0.075 × 0.078 × 0.2	No info	Yes	Yes	No info	Yes	contacting the corresponding author at tangfr@gmail.com	[36]
Turone Mouse Brain Template and Atlas (TMBTA)	analog brain mapping					T2	0.06 × 0.06 × 0.06		Yes	Yes	1327	Yes	https://www.nitrc.org/projects/tmbta_2019	[34]
Duke Mouse Atlas (DMA)	C57BL/6J, DBA/2J, CAST/EiJ, BTBR	4 male and 4 female	90 ± 1 d	Ex vivo	9.4T	DTI	0.045 × 0.045 × 0.045	23.2 h	Yes	Yes	166	No	https://civmvoxport.vm.duke.edu/voxbase/studyhome.php?studyid=402	[37]
The Institute of High Energy Physics Mouse Template (IMT)	C57BL/6J	38 male	10-11w	In vivo	7T	T2	0.06 × 0.05 × 0.2	No info	Yes	Yes	707	Yes	contacting the corresponding author at shanbc@ihep.ac.cn	[31]
Australian Mouse Brain Mapping Consortium (AMBMC)	C57BL/6J	18 male	12w	Ex vivo	16.4T	T1/T2*	0.03 × 0.03 × 0.03	5 h 15 m	Yes	Yes (Partial: diencephalon)	89	No	http://www.imaging.org.au/AMBMC	[38–42]
	C57BL/6J	18 male	12w	Ex vivo	16.4T	T1/T2*	0.03 × 0.03 × 0.03	5 h 15 m	Yes	Yes (Partial: basal ganglia)	35	No		
	C57BL/6J	18 male	12w	Ex vivo	16.4T	T1/T2*	0.03 × 0.03 × 0.03	5 h 15 m	Yes	Yes (Partial: neocortex)	74	No		
	C57BL/6J	18 male	12w	Ex vivo	16.4T	T1/T2*	0.03 × 0.03 × 0.03	5 h 15 m	Yes	Yes (Partial: cerebellum)	38	No		
	C57BL/6J	18 male	12w	Ex vivo	16.4T	T1/T2*	0.03 × 0.03 × 0.03	3 h 40 m	Yes	Yes (Partial: hippocampus)	40	No		
Templates for In vivo Mouse Brain	C57BL/6J, BALB/cBy, C3H/He, DBA/2	30 male 10 male 10 male 10 male	17w	In vivo	7T	T1	0.08 × 0.08 × 0.08	2 h	Yes	No	No info	Yes	http://www.nitrc.org/projects/tpm_mouse	[43]
In vivo MEMRI-based Mouse Brain Atlas	NSG	19 male	1y	In vivo	7T	T1, T2	0.1 × 0.1 × 0.1, 0.1 × 0.1 × 0.1	27 m, 1 h 55 m	No	Yes	41	No	contacting the corresponding author at yutongliu@unmc.edu	[44]
Sawiak_2013	C57BL/6J	82	18w	Ex vivo	4.7T	T2	0.07 × 0.07 × 0.07	3.5 h	Yes	Yes	No info	Yes	contacting the corresponding author at sjs80@cam.ac.uk	[45,46]
Johns Hopkins Medical Institute Laboratory of Brain	C57BL/6J	13 female	2 m, P7–P14	In vivo	11.7T	DTI	0.125 × 0.125 × 0.125	2–2.5 h	Yes	Yes	60	No	https://cmrm.med.jhmi.edu/	[18,19,47]
	C57BL/6J	94	E12 - P80	Ex vivo	11.7T	DTI	0.08 × 0.08 × 0.08–0.125 × 0.125 × 0.125	24 h	Yes	Yes	No info	No		

(*continued on next page*)

Table 1 (*continued*)

Name	Strains	Number of mice	Age	In vivo/ Ex vivo	Field	Contrast	Spatial Resolution (mm^3)	Scan duration	Template	Atlas	Brain structures	GM, WM, CSF priors	Link	Reference (s)
Anatomical MRI	C57BL/ 6J	9 male	140-160d, 7-63d	In vivo, Ex vivo	9.4T, 11.7T	T2, DTI	0.05 × 0.05 × 0.125, 0.0625 × 0.0625 × 0.0625	1 h, 24 h	Yes	Yes	No info	No		
Waxholm Space (WHS)	C57BL/ 6J	No info	9-12w	Ex vivo	9.4T	DTI, T1/T2*	0.043 × 0.043 × 0.043	28 h, 1 h	Yes	Yes	No info	Yes	NITRC: Waxholm Space Atlas of the C57BL/6J Mouse Brain: Tool/ Resource Info	[25,48, 49]
	C57BL/ 6J	14 male	66-78d	Ex vivo	9.4T	T1, T2, T2*	0.0215 × 0.0215 × 0.0215, 0.043 × 0.043 × 0.043, 0.0215 × 0.0215 × 0.0215	No info	Yes	Yes	37	No		
Pre-Waxholm Space	C57BL/ 6J, BXD	12 male	9w	Ex vivo	9.4T	T1, T2	0.0215 × 0.0215 × 0.0215, 0.043 × 0.043 × 0.043	2 h, 4 h	Yes	Yes	20	No	contacting the corresponding author at gaj@ orion.duhs.duke. edu	[50–53]
	C57BL/ 6J	6	9w	Ex vivo	9.4T	T1, T2	0.0215 × 0.0215 × 0.0215, 0.043 × 0.043 × 0.043	2 h 7 m, 4 h 15 m	Yes	Yes	33	No		
	C57BL/ 6J	6 male	9w	Ex vivo	9.4T	T2, PD/ DW	0.09 × 0.09 × 0.09	No info	Yes	Yes	21	No		
	C57BL/ 6J	9 male	No info	Ex vivo	9.4T	T2* DTI	0.039 × 0.039 × 0.156, 0.043 × 0.043 × 0.043	No info	No	No	No info	No		
BNL_NHMFL	C57BL/ 6J	12 male	12-14w	In vivo	9.4T	T2	0.1 × 0.1 × 0.1	2.8 h	Yes	Yes	20	No	https://www.nitrc. org/projects/c57bl_ mr_atlas/	[54,55]
	C57BL/ 6J	10 male	12-14w	Ex vivo	17.6T	T2*	0.047 × 0.047 × 0.047	5.5 h	Yes	Yes	20	No		
Dorr_2008	C57BL/ 6J	20 male and 20 female	12w	Ex vivo	7T	T2	0.032 × 0.032 × 0.032	11.3 h	Yes	Yes	62	No	http://www. mouseimaging.ca/ technologies/ mouse_atlas/index. html	[56,57]
Dorr_2007	CBA	4 male	6–16 m	Ex vivo	7T	T2	0.032 × 0.032 × 0.032	14 h	No	Yes	26	No		
Chen_2006	129S1/ SvImJ, C57BL/ 6J, CD1	27 male	126d	Ex vivo	7T	T2	0.06 × 0.06 × 0.06	18.5 h	Yes	Yes	42	No	contacting the corresponding author at josette@ sickkids.ca	[58,59]

(*continued on next page*)

Table 1 (*continued*)

Name	Strains	Number of mice	Age	In vivo/ Ex vivo	Field	Contrast	Spatial Resolution (mm^3)	Scan duration	Template	Atlas	Brain structures	GM, WM, CSF priors	Link	Reference (s)
Kovacevic_2005	129S1/ SvImJ	9 male	8w	Ex vivo	7T	T2	0.06 × 0.06 × 0.06	No info	Yes	Yes	9	No		
MAP 2003 Atlas	C57BL/ 6J	165 male	100d	In vivo	11.7T	T2	0.06 × 0.06 × 0.06	No info	Yes	Yes	No info	No	contacting the corresponding author at toga@loni.ucla.edu	[60]
Bock_2006	C3H/ HeSnJ	15	11w	In vivo	7T	T1	0.156 × 0.156 × 0.156	2 h 45 m	Yes	Yes	6	No	contacting the corresponding author at bockn@mail.nih.gov	[61]
LONI	C57BL/ 6J	8	P0	Ex vivo	11.7T	T2	0.04 × 0.04 × 0.04	No info	Yes	Yes	12	Yes	contacting the corresponding	[1,62]
	C57BL/ 6J	6 male	100d	In vivo	11.7T	T2	0.06 × 0.06 × 0.06	No info	Yes	Yes	No info	No	author at toga@loni.ucla.edu	

Table 2
Overview of rat MRI brain atlas research (in reverse order of publication time and version).

Name	Strains	Number of mice	Age	In vivo/ Ex vivo	Strength	Contrasts	Spatial Resolution (mm^3)	Scan duration	Template	Atlas	Brain structures	GM, WM, CSF priors	Link	Reference (s)
Hebei Medical University rat brain template set (HRT)	Spontaneously hypertensive rats	8 male	10-52w	In vivo	7T	T2 DTI BOLD	0.137 × 0.137 × 0.3 0.273 × 0.273 × 0.8 0.313 × 0.313 × 0.8	23 m 22 m 7 m	Yes	Yes	163	Yes	https://www.nitrc.org/projects/template_shr	[63]
Duke Rat Atlas	Wistar	6 male	No info	Ex vivo	7T	T2*, DTI	0.025 × 0.025 × 0.025, 0.05 × 0.05 × 0.05	No info	Yes	Yes	360	No	https://civmvoxport.vm.duke.edu/voxbase/studyhome.php?studyid=754	[64]
	Wistar	99 male	0-80d	Ex vivo	7T	T2*, DTI	0.025 × 0.025 × 0.025, 0.05 × 0.05 × 0.05	No info	Yes	Yes	26	No	http://www.civm.duhs.duke.edu/ratbraindevatlas/	[65]
	Wistar	5 male	80d	Ex vivo	7T	T2*	0.025 × 0.025 × 0.05	13 h	Yes	Yes	21	No	contacting the corresponding author at gjohnson@duke.edu	[66,67]
	Fischer 344	1	No info	Ex vivo	1.5T	T1	0.115 × 0.115 × 1.2	No info	Yes	Yes	<2 0	Yes		
Ratlas-LH	Lister hooded	7 male	2–3 m	In vivo	7T	T2	0.15 × 0.15 × 0.15	92 m	Yes	Yes	No info	No	https://www.nitrc.org/projects/ratlas-lham	[68]
Goerzen_2020	Fischer 344	24 male and 17 female	130 ± 7d	In vivo	7T	T2	0.114 × 0.114 × 0.114	19 m 35 s	Yes	Yes	71	Yes	www.zenodo.org/record/3700210	[69]
SIGMA	Wistar	6 male 47 male	8w	Ex vivo, In vivo	11.7T	T2*, T2	0.09 × 0.09 × 0.18, 0.15 × 0.15 × 0.30	8 h 32 m, 14 m 24 s	Yes	Yes	61	Yes	https://nitrc.org/projects/sigma_template	[70]
Waxholm Space (WHS)	Sprague-Dawley	1 male	80d	Ex vivo	7T	T2*, DTI	0.039 × 0.039 × 0.039, 0.078 × 0.078 × 0.078	No info	Yes	Yes (add: auditory system)	118	No	http://www.nitrc.org/projects/whs-sd-atlas	[27–29]
	Sprague-Dawley	1 male	80d	Ex vivo	7T	T2*, DTI	0.039 × 0.039 × 0.039, 0.078 × 0.078 × 0.078	No info	Yes	Yes (add: hippocampal region)	79	No		
	Sprague-Dawley	1 male	80d	Ex vivo	7T	T2*, DTI	0.039 × 0.039 × 0.039,	No info	Yes	Yes	76	No		

(*continued on next page*)

Table 2 (*continued*)

Name	Strains	Number of mice	Age	In vivo/ Ex vivo	Strength	Contrasts	Spatial Resolution (mm^3)	Scan duration	Template	Atlas	Brain structures	GM, WM, CSF priors	Link	Reference (s)
RatAtlas2.0	Long-Evans	2 male	135d	Ex vivo	14.1T	T2	0.078 × 0.078 × 0.078 0.05 × 0.05 × 0.2	10 h	Yes	Yes	No info	No	https://figshare.com/articles/RatAtlas_2_0_Locked_pdf/3144955	[71]
Figini	Sprague-Dawley	10 female	No info	In vivo	7T	T2, DTI	0.133 × 0.133 × 0.58, 0.176 × 0.176 × 0.58	16 m 24 s	No	Yes	28	No	contacting the corresponding author at ileana.zucca@istituto-besta.it	[72]
Lancelot_2014	Sprague-Dawley	7	No info	In vivo	7T	T2	0.1 × 0.1 × 0.4	53 m	No	Yes	27	No	contacting the corresponding author at costes@cermep.fr	[73]
Rumple_2013	Sprague-Dawley	6 female 10 male and 10 female	72d 5-14d	Ex vivo	9.4T	DTI	0.16 × 0.125 × 0.16 0.12 × 0.07 × 0.12	No info	Yes	Yes	29	Yes	https://www.nitrc.org/projects/dti_rat_atlas/	[74]
The Institute of High Energy Physics Rat Template (IRT)	Sprague-Dawley	12 male and 9 female	10-11w	In vivo	7T	T2	0.14 × 0.14 × 0.3	No info	Yes	Yes	624	No	contacting the corresponding author at shanbc@ihep.ac.cn	[75]
Tohoku	Wistar	30 male	10w	In vivo	7T	T2	0.125 × 0.125 × 0.3	3 h	Yes	Yes	96	Yes	contacting the corresponding author at riera@idac.tohoku.ac.jp	[76]
Veraart_2011	Sprague-Dawley	9 male	12 m	In vivo	9.4T	DTI	0.088 × 0.088 × 0.088	4 h	Yes	Yes	14	No	contacting the corresponding author at Jelle.Veraart@ua.ac.be	[77]
Schwarz (DPABI)	Sprague-Dawley	97 male	No info	In vivo	4.7T	T2	0.15 × 0.15 × 1	No info	Yes	Yes	39	Yes	contacting the corresponding author at adam.j.schwarz@gsk.com	[30]
Karolinska	Sprague-Dawley	5 female	No info	In vivo	4.7T	T2	0.117 × 0.117 × 0.5	No info	Yes	Yes	28	No	contacting the corresponding author at christian.spenger@neuro.ki.se	[2]

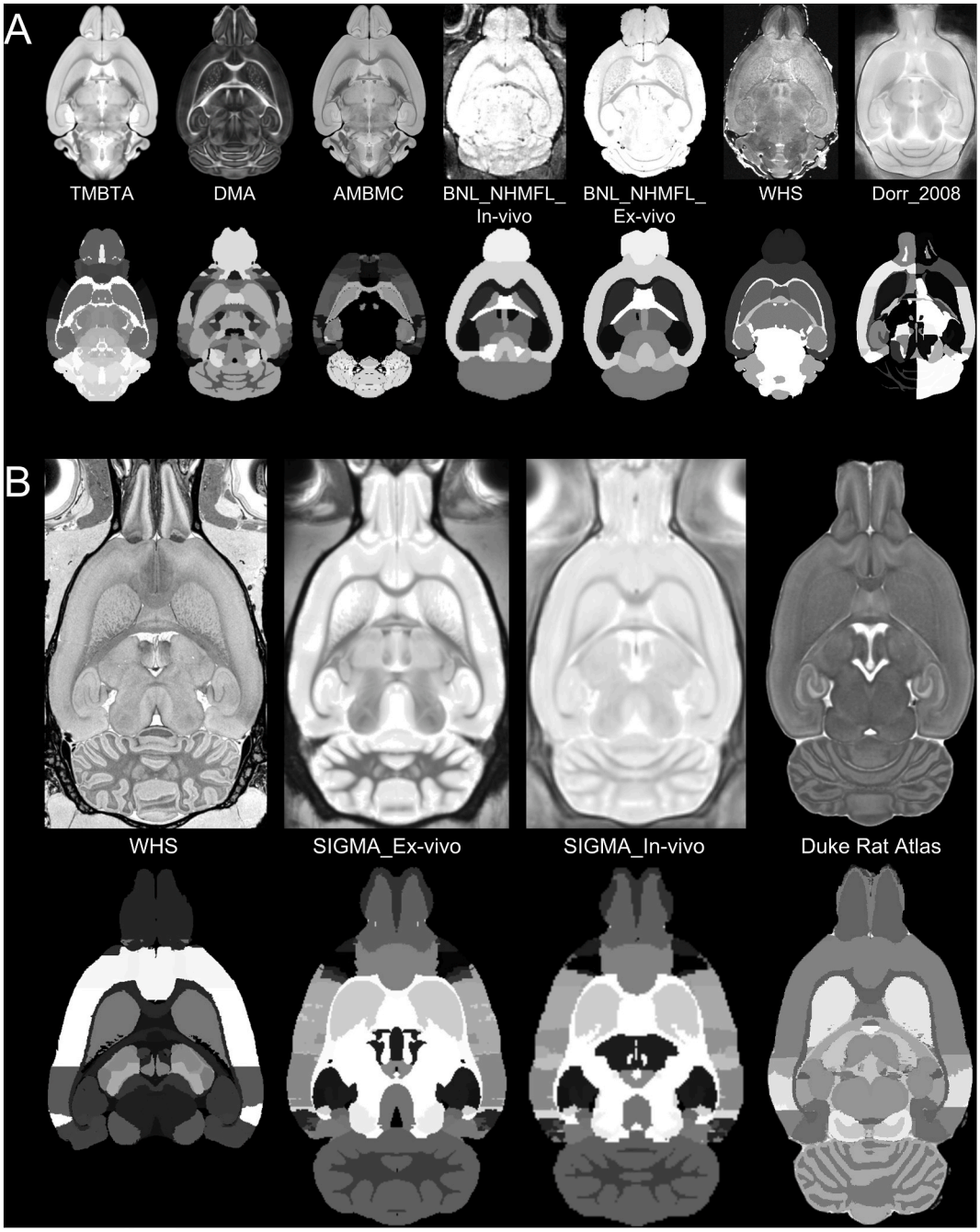

Fig. 1. Transverse views of common mouse and rat brain atlases.
(A) Mouse brain atlases (upper row) and corresponding level of detail of segmented brain regions. **(B)** Rat brain atlases (upper row) and corresponding level of detail of segmented brain regions.

high-resolution population brain template with detailed structural segmentation and annotation. However, the existence of numerous versions of MRI brain atlases compared to histological atlases poses challenges, as there is a lack of standardized anatomical boundaries. This limitation hampers direct comparisons between analysis results based on different versions of MRI brain atlases. To assist researchers in selecting an appropriate MRI brain atlas for their studies and to facilitate future advancements in creating high-quality MRI brain atlases, this paper systematically examines the development and progress achieved in mouse and rat MRI brain atlases.

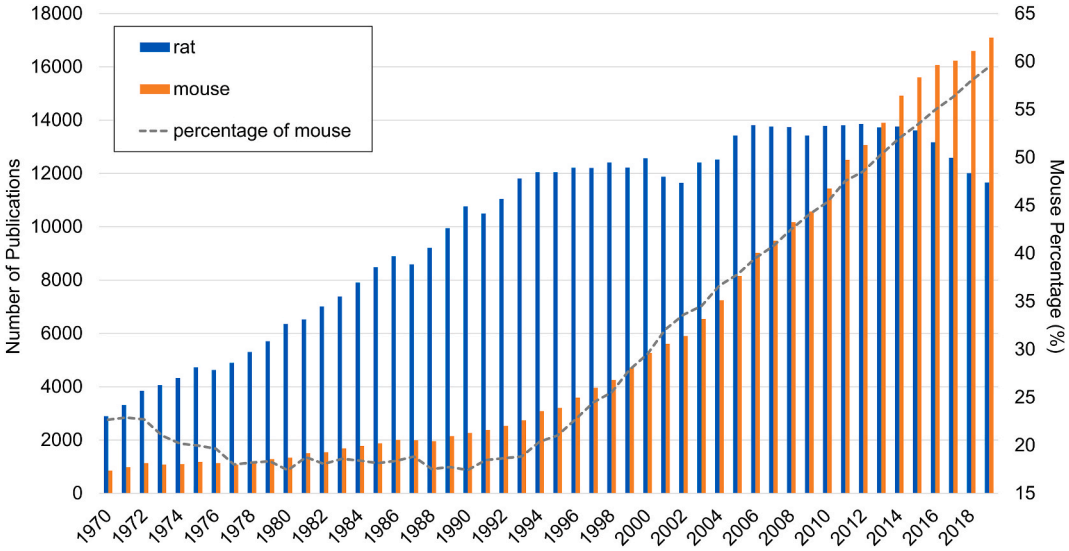

Fig. 2. Mouse and Rat Publications in Neuroscience.
We searched the total number of mouse and rat neuroscience papers published over the past 50 years through Pubmed (https://pubmed.ncbi.nlm.nih.gov). To avoid the possible impact of novel coronavirus pneumonia (COVID-19) on the publication of papers, we advanced the retrieval period from 1970 to 2019. The literature search terms for mouse and rat were ((brain) OR (neuroscience) OR (central nervous system)) AND (mouse) AND (1960:2019[pdat]), and ((brain) OR (neuroscience) OR (central nervous system)) AND (rat) AND (1960:2019[pdat]).

2. The development of mouse and rat MRI brain atlases

In the field of neuroscience research, rats have historically served as the predominant animal model for over a century. Nonetheless, a shift has occurred in recent years, whereby mice have rapidly emerged as the primary choice for such studies, surpassing rats (Fig. 2). This transition can be attributed primarily to the extensive availability of genetic toolboxes for mouse models, particularly with the advancements in gene targeting techniques utilizing embryonic stem cells [78]. Conversely, the manipulation of genes in rats poses greater challenges compared to mice, thus limiting the utility of rats as a rodent model in neuroscience research [79].

Fortunately, with the advent of gene editing techniques suitable for rats and the elucidation of rat genome functions in recent years [80–83], the development of transgenic rat models is progressing rapidly. Although mice and rats are similar in many ways, there are fundamental differences between these rodents, such as the differential expression of more than 40% of genes in the dendrites of hippocampal neurons [84], Opposed responses have been shown in some basic neuroscience research on cognition, addiction, impulsivity, and social behavior [32]. Moreover, with the development and widespread application of brain imaging techniques such as MRI and PET to assess the extent and course of neurodegeneration, rats are more suitable for applying these techniques due to their relatively large size [32]. In addition, compared to mice, the physiological characteristics of rats are closer to those of humans [85]. Therefore, although mouse models have many advantages in neuroscience research, such as low cost of breeding and feeding, low drug consumption in pharmaceutical research, and a complete set of gene editing libraries, rats are still indispensable model animals in neuroscience research.

The indispensability of brain atlases in neuroscience research is derived from their provision of a standardized map and ontology that facilitates the comparison of findings, enabling researchers to gain insights into brain structure, function, and related pathologies. Moreover, these atlases serve as crucial navigation tools, establishing a vital link for in vivo investigations in the field of neuroscience. With the advent of MRI, it is now possible to see the brain within the skull in its natural state without distortion or the introduction of physical artifacts like fixation, dissection, or sectioning. As early as 1995, the first work about mouse brain structure based on MRI was published [86], and then the first MRI-based mouse brain atlas with certain practicality was published in 2004 [1]. Nearly 30 versions of the mouse MRI brain atlas have been published (Table 1). We can see that these previous researches were mainly developed based on adult male C57BL/6J mice. Among them, the highest spatial resolution based on ex vivo and in vivo mouse brain tissue is 0.0215 × 0.0215 × 0.0215 (mm^3) [25,50,51], and 0.05 × 0.05 × 0.125 (mm^3) [18], respectively. The most widely used of these mouse MRI brain atlases are the 129S1/SvImJ mouse brain atlas published by Kovacevic, N. in 2005 [59], and the CBA mouse brain atlas published by Dorr, A. in 2006 [57], and the C57BL/6J mouse brain atlases published by Ma, Y., Dorr, A. E., and Johnson, G. A. in 2005, 2008, and 2010 [25,55,56], respectively. The five versions of the brain atlas were all generated from ex vivo mouse brain tissue, and their number of brain structures ranged from 9 to 62.

Although the development of the rat MRI brain atlas predates the mouse [67], the subsequent continued development of the rat MRI brain atlas has significantly lagged behind that of the mouse (Table 2). As can be seen from the table, the rat MRI brain atlas was developed primarily based on adult male Sprague-Dawley and Wistar rats. Among them, the highest spatial resolution of MR images based on ex vivo and in vivo rat brain tissue is 0.025 × 0.025 × 0.025 (mm3) [64–66], and 0.088 × 0.088 × 0.088 (mm^3) [77],

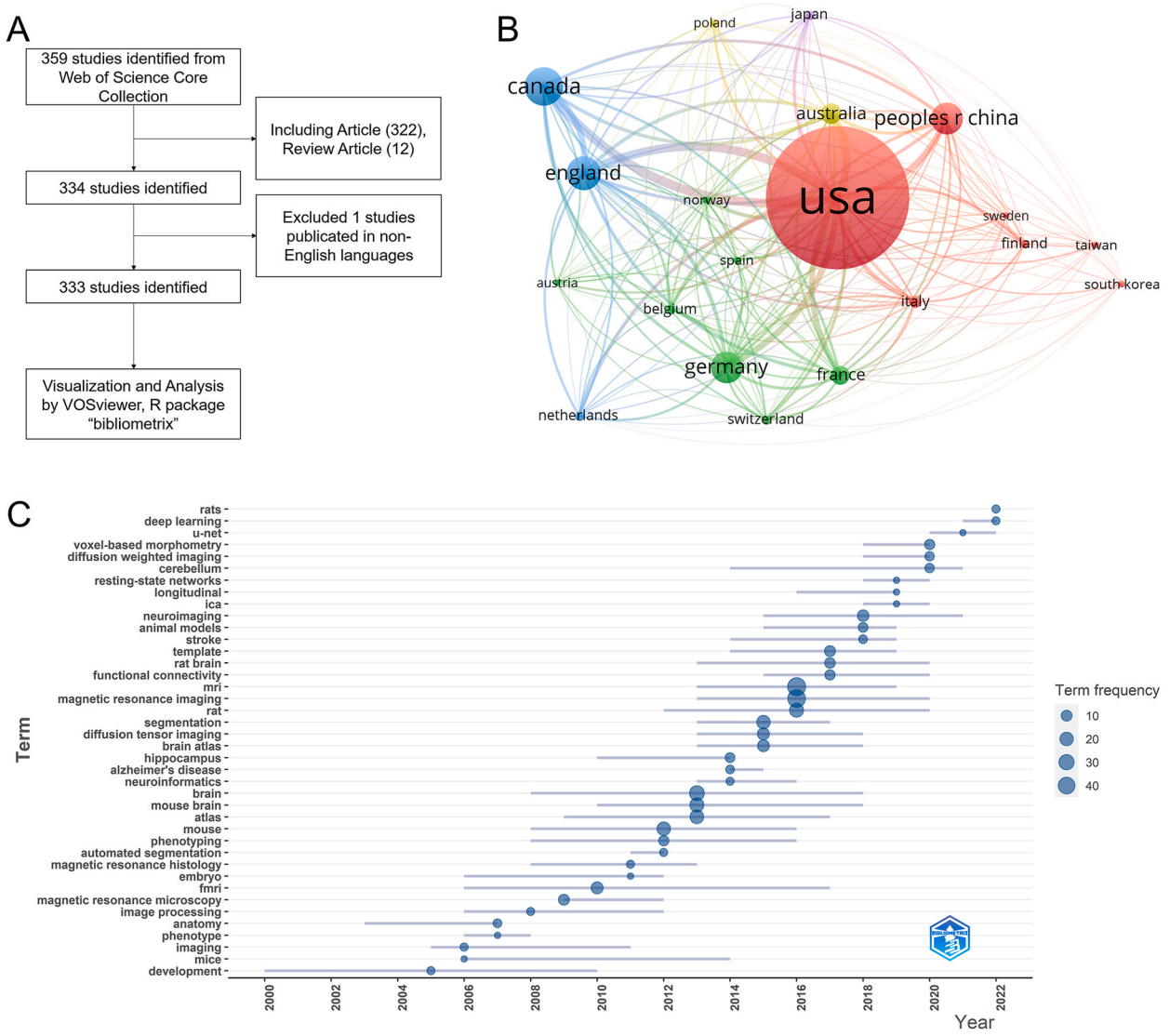

Fig. 3. A bibliometric analysis of rodent MRI-based brain atlases.
(A) Publications screening flowchart. We conducted a literature search on the Web of Science Core Collection (WoSCC) database on December 4, 2022. The search formula is (((TS=(Magnetic Resonance Imaging)) AND TS=((brain atlas) or (brain template))) AND TS=(mouse or rat or rodent) AND LA = (English), and the type of documents is set to "articles" and "review". A total of 359 literature sources were retrieved, including 322 research papers and 12 review articles. After excluding one non-English paper, there were a final count of 333 English-language articles remaining. To conduct bibliometric analysis on these articles, VOSviewer and the R package "bibliometrix" were utilized. **(B)** The visualization of countries in this research field by VOSviewer. **(C)** Trend topic analysis in this field by R package "bibliometrix".

respectively. The most widely used of these rat brain atlases are the Schwarz (DPABI) and Waxholm 1.0 atlases, published by Schwarz, A. J. and Papp, E. A. in 2006 and 2014, respectively [29,30]. Moreover, the Waxholm map was subsequently updated by Kjonigsen, L. J. and Osen, K. K. in 2015 and 2019, respectively [27,28]. The number of brain structures in these rat MRI brain atlases ranged from 39 to 118, significantly more than that in the mouse MRI brain atlases.

Furthermore, through bibliometric analysis, we found that the United States was the global center for MRI brain atlas research in mice and rats over the past 20+ years (Figs. 3A and 2B). Topic trend analysis shows that before 2013, researches mainly focused on mouse brain structure, especially mouse models. From 2014 to 2020, the study of brain function based on rat disease models has become a hotspot; and from 2021 to 2022, the deep learning of MRI brain images based on rat models has become the latest research hotspot (Fig. 3C).

3. The production process of mouse and rat MRI brain atlases

Spatial resolution and contrast of MR images are two key features commonly used to compare the quality of MRI brain atlases [64]. The use of MRI brain atlases is ultimately determined by these two significant, linked aspects. For resolving tiny structures in the brain, high-quality MR picture contrast and spatial resolution are essential. Although various image contrasts may be used to create MRI brain maps, doing so significantly lengthens the time needed to collect all of the necessary high-resolution MR image data and raises the possibility of specimen deterioration and instrument instability, rendering the proposal unfeasible. Consequently, the choice of image contrast for making an atlas may be related to the intended use of the brain atlas. For instance, if you are evaluating PET or MRI brain imaging data in rodent, the T2 template is often included in the atlas [87,88]. The majority of existing mouse and rat MRI brain atlases are based on T2 or T2* sequences shown in Tables 1 and 2, as they provide better tissue contrast for delineating brain structures in adult mice and rats [25,70]. A high-resolution MRI would take longer to scan but would not be practicable. Clinically, the resolution of MRI maps of the adult human brain is usually smaller than 1 mm isotropic. The average volume of the adult human brain is about 3000 times that of the adult mouse [89] and about 700 times that of the rat [90,91]; thus, the comparable resolution of mouse and rat MRI brain images is approximately smaller than 0.07 and 0.11 mm isotropic, respectively.

An important area of study is the creation of new technologies that may enhance the contrast and resolution of MR images. For instance, compared to standard T2 imaging, multispectral MR capture with enhanced T2 contrast in stained pictures may show greater information in mouse brain morphology [57,62]. With the use of partial k-space acquisition and contrast agents (such as for short tissue T1) [50], it can be achieved that MR images of the mouse brain with isotropic resolution up to 21.5 μm [92]. Furthermore, diffusion tensor imaging (DTI) can reveal tissue microstructure through endogenous contrast [93], where axonal protrusions and myelination levels have an impact on how anisotropy is expressed [94], and data on directional and diffusional anisotropy may be utilized to rebuild 3D white matter tract trajectories [95,96]. DTI also has the key benefit of being able to better contrast the structure of young mouse brain tissue than T1 and T2 MRI [97,98]. Moreover, a similar phenomenon also exists in rats [65]. Therefore, DTI is a critical MRI technique for developing brain atlases in young mice and rats.

A comprehensive MRI brain mapping protocol typically encompasses the inclusion of brain templates, digital brain atlases, and probability maps representing gray matter, white matter, and cerebrospinal fluid. The procedure entails several steps: firstly, a sample set comprising 10–30 rodent brain tissues of the same sex and age is prepared, with the possibility of employing ex vivo tissues treated with contrast agents like Gd^{3+} or Mn^{2+}. Subsequently, the samples are scanned using high-field MRI equipment such as 7.0T, 9.4T, or 11.4T to acquire T2, T2*, and DTI MR images. Following this, a brain template is constructed by generating a population-averaged

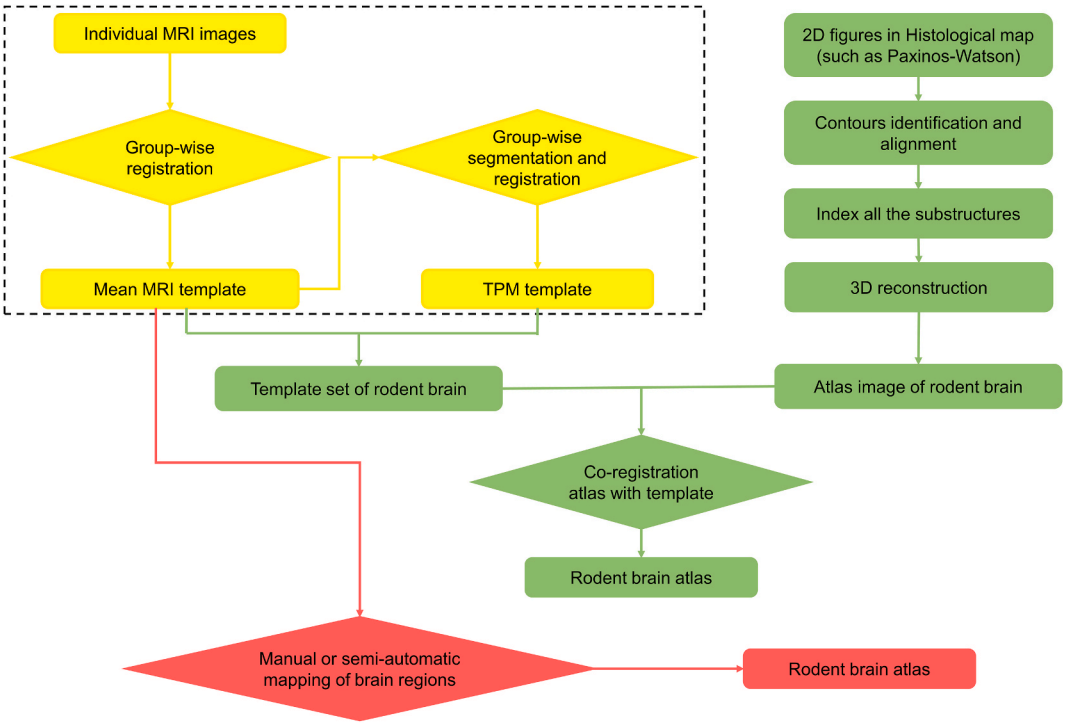

Fig. 4. Flow chart of mouse and rat MRI brain map.
This figure presents two flowcharts depicting the creation of brain maps. The first flowchart, highlighted in green, illustrates the automated generation of a brain map using histology atlases. The second flowchart, highlighted in red, outlines the process of drawing a brain atlas based on a brain template. Additionally, the yellow section (in the dotted box) represents the shared components between these two methods. TMP, tissue probability maps.

template from multiple sample images. Probability maps for different brain compartments, including cerebrospinal fluid, white matter, and gray matter, are then developed. Furthermore, a digital brain atlas is created by manually or semi-automatically mapping brain structures and aligning them with standard coordinate spaces, such as Paxinos-Watson atlas. Finally, the automatic analysis of brain images can be achieved. Fig. 4 illustrates the two main pipelines utilized for the development of MRI brain atlases in mice and rats.

4. Application of mouse and rat MRI brain atlases

4.1. Studies on brain histomorphology and multimodal approaches

In the field of neuroscience, studying brain histomorphology is essential for understanding the structure and function of the brain. Histomorphology refers to the measurement and analysis of changes in the size and form of various anatomical regions within the brain. Traditionally, this process has been performed through manual delineation of structures in consecutive MR images. However, this approach is time-consuming and prone to variations in the determination of anatomical boundaries and inter-rater variability [99]. The issue of operator-dependent results poses a significant challenge in neuroscience research. Different operators may have different interpretations or methodologies when it comes to defining anatomical structures, leading to inconsistencies across studies and limiting comparability between different laboratories [100]. This lack of compatibility hampers scientific progress and makes it difficult to draw meaningful conclusions from collective findings.

To address these challenges, advances in image registration and mapping techniques, as well as the development of brain atlases, offer promising solutions [101]. Image registration methods allow for aligning multiple brain images, enabling direct comparisons between subjects or datasets. By aligning different brain images to a common coordinate system, researchers can accurately measure and compare morphological changes in specific brain regions. Furthermore, the availability of brain atlases provides standardized reference frameworks that facilitate the identification and localization of anatomical structures. These atlases serve as templates or maps that can be overlaid onto individual brain images, aiding in the accurate identification and delineation of specific regions of interest. By leveraging image registration techniques and using brain atlases, researchers can overcome the limitations associated with manual delineation and achieve more consistent and reliable measurements of brain morphology. This standardization improves the reproducibility of results, enhances cross-study comparisons, and fosters collaboration among different research groups. Moreover, with the development of multimodal image registration technology, the integration of data from other brain imaging modalities (such as 3D histology, sliced brain connection maps, and brain tissue transparent imaging) into MRI brain atlases may facilitate investigations of network alterations underlying neurological disorders [102].

4.2. Multimodal brain imaging data analysis

With the development of imaging techniques, such as MRI and PET, these techniques are being increasingly applied in basic neuroscience research. Compared with traditional brain tissue detection tools, imaging technology has unparalleled advantages in non-invasive detection. In addition to the above-mentioned structural imaging of brain tissue, the detection of brain function at the molecular level can also be achieved by combining molecular probes. Table 3 lists common application scenarios that need combining with a brain atlas for data analysis. Such as, imaging techniques have been employed to longitudinally monitor brain development in mouse models [103,104]. Additionally, the combination of chemical genetics and brain functional imaging techniques has facilitated the investigation of brain chemical connectomics in mice [105,106]. Moreover, the utilization of superparamagnetic iron oxide nanoparticles (SPION) has enabled quantitative imaging of cerebral blood vessels in mice, thereby facilitating further exploration of brain function [107]. Furthermore, the analysis of glucose energy metabolism in brain tissue has provided insights into the metabolic status of different brain regions [108,109]. Lastly, the deposition of pathological proteins in mouse brain tissue has been detected using Aβ protein or tau protein probes [110,111]. These examples represent only a fraction of the wide range of applications that could benefit from the fusion of a brain atlas with brain imaging.

Table 3
Common application scenarios for brain image data analysis based on brain atlas.

Image modality	Imaging sequence or molecular probe	The role of imaging	Reference
MRI	T2, DTI	Assess brain development	[103,104]
MRI	T2, BOLD	Brain chemical connectomics research	[105,106]
MRI	T1 (SPION)	Cerebral vascular quantitative imaging	[107]
MRI	T1 (MnCl2)	MEMRI maps	[112]
MRI	CBV, BOLD	Brain functional network under conditioned stimulation	[113]
MRI	T2 (Gd)	Blood-brain barrier permeability test	[114]
PET	18F-FDG	Detection of energy metabolism in brain tissue	[108,109]
PET	18F-florbetaben, 11C-PBB3	Detection of pathological proteins, such as Aβ protein and tau protein	[110,111]
PET	11C-raclopride	Detection of neurotransmitter receptors, such as dopamine D2 receptors	[115]
PET	18F-FDG	Neural circuit research	[116]

4.3. CT-MRI combined brain atlas for guiding stereotaxic manipulation

The precision of the brain atlas utilized in stereotaxic surgery for targeting structures in the mouse and rat brain directly impacts the accuracy of interventions. While 2D histology-based atlases are commonly used to localize brain regions based on stereoscopic coordinates relative to calvarial landmarks, MRI-based mouse and rat brain atlases provide anatomical information but lack the bone tissue contrast necessary for recognizing cranial landmarks critical for stereotaxic procedures. To address this limitation, the combination of MR and micro-CT images has been employed to develop 3D stereotaxic mouse brain atlases (CT-MRI brain atlas) [18,117]. However, the development of corresponding rat brain atlases using this approach has not been reported. It is worth noting that atlases generated using ex vivo specimens may not accurately represent the true architecture of the live animal brain, further emphasizing the need for accurate targeting during stereotaxic surgeries.

CT-MRI atlases, despite their limited anatomical detail compared to histology-based atlases, are valuable for stereotaxic-related applications due to their ability to visualize brain anatomy in 3D. This enables precise determination of target coordinates, injection angles, and simulation of needle paths, thereby avoiding damage to adjacent brain structures. Additionally, these atlases offer the flexibility to rotate and slice in various orientations beyond the conventional bregma-lambda coordinate system, allowing redefinition of stereo coordinates relative to user-specified landmarks. Consequently, experimental animal surgeries benefit from enhanced surgical operation flexibility and avoidance of inadvertent harm to critical neighboring structures.

5. Aeras for improvement of mouse and rat MRI brain atlases

In recent years, significant advancements have been made in the development of MRI brain atlases for mice and rats, paralleling the rapid progress of MRI technology. Notably, the spatial resolution of voxels has reached an impressive level of less than 100 μm isotropic. However, despite these remarkable achievements, there still exist several areas that warrant further improvement, as outlined in Table 4. One key concern is the absence of a universally accepted and standardized version of these atlases, hindering effective collaboration and comparison among researchers. Moreover, the lack of high-quality in vivo brain atlases, particularly for mice, poses a significant challenge in accurately characterizing the dynamic nature of the brain. Additionally, the current atlases predominantly focus on male animals, neglecting the need for brain atlas versions specifically tailored to female subjects. Furthermore, the dearth of brain atlases for different age groups restricts our understanding of developmental changes and potential age-related differences in brain structures. Addressing these limitations would greatly enhance the utility and applicability of mouse and rat MRI brain atlases, ultimately promoting the widespread application of brain imaging technology in the field of neuroscience research.

6. Summary and perspective

Significant advancements have been made in the development of both histological brain atlases and MRI brain atlases since the inception of early histological atlases. A recent milestone includes the practical development of a 3D mouse brain atlas based on histological data [13]. Furthermore, digital atlases derived from multi-sequence data have emerged in the field of MRI brain atlases, enabling the mapping of a larger number of brain regions with higher precision [64]. The efficacy of brain atlases relies on the inclusion of high-resolution anatomical images that exhibit rich anatomical contrast and precise structural delineation. In histology-based mouse and rat brain atlases, manual outlining of brain structures on stained tissue section photographs is commonly performed, leveraging knowledge of specific cellular and molecular markers as well as spatial correlations. Conversely, MRI-based mouse and rat brain atlases often employ structure segmentation in 3D images, where voxels belonging to a particular structure are identified and classified as distinct 3D entities due to the inherent 3D format of these images. Additionally, the segmentation of brain MR images is frequently accomplished through manual [18,56] or semi-automatic techniques [52,58].

The conventional approach to producing brain atlases typically involves utilizing one or a limited number of specimens. However, with the rapid advancements in computer technology, it has become feasible to spatially normalize and average MRI 3D images obtained from multiple specimens. These techniques can also be employed to generate “minimum deformation maps” that resemble the geometric mean of a normal brain, capturing the representative morphological characteristics of the sample population [40]. The

Table 4
Aeras for improvement of mouse and rat MRI brain atlases.

Atlas category	Aeras for improvement
Mouse	• Lack of unified version • Lack of versions based on in vivo tissue • Lack of versions based on female tissue • Lack of mouse brain atlas at different ages • Limitations in the precise delineation of brain structures
Rat	• Lack of unified version • Too few samples to make some versions • Lack of versions based on female tissue • Lack of rat brain atlas at different ages • No CT-MRI combined brain atlas • Limitations in the precise delineation of brain structures

utilization of averaged images enhances the signal-to-noise ratio compared to individual images, facilitating easier structural segmentation and visualization of brain atlases through group averaging [40].

The majority of existing MRI brain atlas images are derived from ex vivo samples as they offer a simpler means to generate high-resolution images compared to in vivo samples. Ex vivo specimens, typically fixed with formaldehyde, can be trimmed to match the optimal shape for sensitive MR coils, allowing the creation of excellent MR images through the combination of these specimens with high-performance gradient systems [25]. However, this optimized imaging hardware combination is generally unsuitable for in vivo MRI due to increased requirements for animal monitoring and support systems. Moreover, ex vivo MRI scanning sessions can extend up to 12 h or more, enabling further improvement in MR image quality through increased signal averaging [66]. Conversely, in vivo imaging may suffer from motion artifacts or instability, with scanning times typically limited to 2–3 h [19,76]. Given these characteristics, ex vivo imaging represents the superior method for acquiring high-quality MR images of the mouse and rat brain.

The limitations of in vivo MRI are primarily attributed to the sensitivity of the imaging device and the duration for which an anesthetized animal can remain stable within the magnet. However, if the intended use of the atlas is to evaluate brain images of live animals, the development of an in vivo MRI-based atlas becomes essential, despite the aforementioned disadvantages associated with in vivo MRI. It has been observed that MR image contrast and appearance differ between in vivo and ex vivo tissues, likely due to changes in the physical and chemical environment surrounding water molecules caused by fixation [118]. Additionally, significant morphological differences exist between live animal brains and perfusion-fixed brain specimens. For instance, the absence of cerebrospinal fluid (CSF) pressure often leads to a notable reduction or complete collapse of the lateral ventricles in postmortem specimens [54,101]. Additionally, when studying ex vivo brains, the removal of blood results in collapsed vasculature and consequent brain shrinkage [54,101]. Moreover, the brain tissue may furthermore slightly expand or contract depending on the osmolarity of the fixative solution [119,120]. Therefore, it is necessary to vigorously develop MRI brain atlases based on in vivo samples in the future, especially MRI brain atlases of living mice. Moreover, in the foreseeable future, 7.0T, 9.4T, and 11.7T will still be the mainstream scanning devices for small animal in vivo.

With the development of molecular imaging technology, in vivo animal brain imaging technology will be more and more used in neuroscience research. However, compared to histological brain atlases, there is still a lack of uniform standard mouse and rat MRI brain atlases. It is crucial to understand the variations that can arise between different atlases and their versions. We would like to highlight the work of Kleven et al. and their proposed Atlas Ontology Model (AtOM), which may offer a solution to the lack of standardization in metadata, enabling improved analysis, data sharing, and registration across different atlases [121]. In addition, the easier acquisition of MR images makes it possible to develop rodent MRI brain atlases of different strains, genders, and ages, which will further promote the application of MRI-based brain atlases. Finally, creating a CT-MRI combined brain atlas is also of great value to ensure the reliability of the manipulation of rodent brain surgery.

In summary, the MRI brain atlas is an ongoing endeavor that continuously strives for improvement and increased precision. Future enhancements to brain atlases may involve the incorporation of machine learning or other automated methods, alleviating the labor-intensive human involvement required in current iterations. Furthermore, the evolution of brain atlases is expected to progress from the existing structure map towards a more comprehensive structure-function integration map.

Funding

This work was supported financially by the National Natural Science Foundation of China (No. 81901304 to Dr. Huanhuan Yan) and the Guangdong Basic and Applied Basic Research Foundation (No. 2021A1515110199 to Dr. Xiaoyi Ma).

Data availability statement

Data included in article/supp. material/referenced in article.

CRediT authorship contribution statement

Xiaoyi Ma: Writing – original draft. **Yao Xing:** Writing – original draft. **Renkuan Zhai:** Supervision. **Yingying Du:** Supervision. **Huanhuan Yan:** Writing – review & editing, Writing – original draft, Supervision.

Declaration of competing interest

The authors declare that they have no known competing financial interests or personal relationships that could have appeared to influence the work reported in this paper.

References

[1] A. MacKenzie-Graham, et al., A multimodal, multidimensional atlas of the C57BL/6J mouse brain, J. Anat. 204 (2) (2004) 93–102.
[2] P. Schweinhardt, P. Fransson, L. Olson, C. Spenger, J.L. Andersson, A template for spatial normalisation of MR images of the rat brain, J. Neurosci. Methods 129 (2) (2003) 105–113.
[3] G. Paxinos, K.B. Franklin, The Mouse Brain in Stereotaxic Coordinates. *Third*, Academic Press, 2008.
[4] B.M. Slotnick, C.M. Leonard, A Stereotaxic Atlas of the Albino Mouse Forebrain, vol. 75, US Department of Health, Education, and Welfare, Public Health Service, 1975.

[5] P.R. Hof, Comparative Cytoarchitectonic Atlas of the C57BL/6 and 129/Sv Mouse Brains, Elsevier, 2000.
[6] C. Watson, G. Paxinos, Chemoarchitectonic Atlas of the Mouse Brain, Academic, 2010.
[7] G. Paxinos, K.B. Franklin, Paxinos and Franklin's the Mouse Brain in Stereotaxic Coordinates, Academic press, 2019.
[8] G. Paxinos, Paxinos and Watson's the Rat Brain in Stereotaxic Coordinates, Elevier Academic Press, 2014.
[9] L.W. Swanson, Brain Maps: Structure of the Rat Brain, first ed. ed, Elsevier, Amsterdam, The Netherlands, 1992.
[10] L. Swanson, Brain Maps: Computer Graphics Files, 1992. Amsterdam.
[11] L.W. Swanson, Brain maps 4.0-Structure of the rat brain: an open access atlas with global nervous system nomenclature ontology and flatmaps, J. Comp. Neurol. 526 (6) (2018) 935–943.
[12] S.W. Oh, et al., A mesoscale connectome of the mouse brain, Nature 508 (7495) (2014) 207–214.
[13] Q. Wang, et al., The allen mouse brain common coordinate framework: a 3D reference atlas, Cell 181 (4) (2020) 936–953 e20.
[14] L.J. Pellegrino, A.J. Cushman, Stereotaxic Atlas of the Rat Brain, 1967.
[15] E.L. Simson, A.P. Jones, R.M. Gold, Horizontal stereotaxic atlas of the albino rat brain, Brain Res. Bull. 6 (4) (1981) 297–326.
[16] F. Valverde, F. Valverde, Golgi Atlas of the Postnatal Mouse Brain, Springer, 1998.
[17] D.M. Simmons, L.W. Swanson, Comparing histological data from different brains: sources of error and strategies for minimizing them, Brain Res. Rev. 60 (2) (2009) 349–367.
[18] M. Aggarwal, J. Zhang, M.I. Miller, R.L. Sidman, S. Mori, Magnetic resonance imaging and micro-computed tomography combined atlas of developing and adult mouse brains for stereotaxic surgery, Neuroscience 162 (4) (2009) 1339–1350.
[19] D. Wu, et al., In vivo high-resolution diffusion tensor imaging of the mouse brain, Neuroimage 83 (2013) 18–26.
[20] A.W. Toga, M. Samaie, B.A. Payne, Digital rat brain: a computerized atlas, Brain Res. Bull. 22 (2) (1989) 323–333.
[21] G. Paxinos, Paxinos & Watson the Rat Brain in Stereotaxic Coordinates: the New Coronal Set, Elsevier, 2005.
[22] J.-P. Konsman, The mouse brain in stereotaxic coordinates-(Deluxe) by Paxinos G. and Franklin, KBJ, Academic Press, New York, 2001, Psychoneuroendocrinology 6 (28) (2003) 827–828. SBN *0-12-547637-X*.
[23] P. Majka, E. Kublik, G. Furga, D.K. Wojcik, Common atlas format and 3D brain atlas reconstructor: infrastructure for constructing 3D brain atlases, Neuroinformatics 10 (2) (2012) 181–197.
[24] U. Chon, D.J. Vanselow, K.C. Cheng, Y. Kim, Enhanced and unified anatomical labeling for a common mouse brain atlas, Nat. Commun. 10 (1) (2019) 5067.
[25] G.A. Johnson, et al., Waxholm space: an image-based reference for coordinating mouse brain research, Neuroimage 53 (2) (2010) 365–372.
[26] J.F. Ullmann, A.L. Janke, D. Reutens, C. Watson, Development of MRI-based atlases of non-human brains, J. Comp. Neurol. 523 (3) (2015) 391–405.
[27] K.K. Osen, J. Imad, A.E. Wennberg, E.A. Papp, T.B. Leergaard, Waxholm Space atlas of the rat brain auditory system: three-dimensional delineations based on structural and diffusion tensor magnetic resonance imaging, Neuroimage 199 (2019) 38–56.
[28] L.J. Kjonigsen, S. Lillehaug, J.G. Bjaalie, M.P. Witter, T.B. Leergaard, Waxholm Space atlas of the rat brain hippocampal region: three-dimensional delineations based on magnetic resonance and diffusion tensor imaging, Neuroimage 108 (2015) 441–449.
[29] E.A. Papp, T.B. Leergaard, E. Calabrese, G.A. Johnson, J.G. Bjaalie, Waxholm space atlas of the Sprague dawley rat brain, Neuroimage 97 (2014) 374–386.
[30] A.J. Schwarz, et al., A stereotaxic MRI template set for the rat brain with tissue class distribution maps and co-registered anatomical atlas: application to pharmacological MRI, Neuroimage 32 (2) (2006) 538–550.
[31] B. Nie, et al., A stereotaxic MRI template set of mouse brain with fine sub-anatomical delineations: application to MEMRI studies of 5XFAD mice, Magn. Reson. Imaging 57 (2019) 83–94.
[32] B. Ellenbroek, J. Youn, Rodent models in neuroscience research: is it a rat race? Dis Model Mech 9 (10) (2016) 1079–1087.
[33] N. Verbeeck, et al., Connecting imaging mass spectrometry and magnetic resonance imaging-based anatomical atlases for automated anatomical interpretation and differential analysis, Biochim. Biophys. Acta Protein Proteonomics 1865 (7) (2017) 967–977.
[34] D.A. Barriere, et al., Brain orchestration of pregnancy and maternal behavior in mice: a longitudinal morphometric study, Neuroimage 230 (2021) 117776.
[35] G.-P. Yan, L. Robinson, P. Hogg, Magnetic resonance imaging contrast agents: overview and perspectives, Radiography 13 (2007) e5–e19.
[36] B.X. Ren, et al., Early postnatal irradiation-induced age-dependent changes in adult mouse brain: MRI based characterization, BMC Neurosci. 22 (1) (2021) 28.
[37] N. Wang, et al., Variability and heritability of mouse brain structure: microscopic MRI atlases and connectomes for diverse strains, Neuroimage 222 (2020) 117274.
[38] C. Watson, et al., An ontologically consistent MRI-based atlas of the mouse diencephalon, Neuroimage 157 (2017) 275–287.
[39] J.F. Ullmann, et al., An MRI atlas of the mouse basal ganglia, Brain Struct. Funct. 219 (4) (2014) 1343–1353.
[40] J.F. Ullmann, C. Watson, A.L. Janke, N.D. Kurniawan, D.C. Reutens, A segmentation protocol and MRI atlas of the C57BL/6J mouse neocortex, Neuroimage 78 (2013) 196–203.
[41] J.F. Ullmann, et al., Segmentation of the C57BL/6J mouse cerebellum in magnetic resonance images, Neuroimage 62 (3) (2012) 1408–1414.
[42] K. Richards, et al., Segmentation of the mouse hippocampal formation in magnetic resonance images, Neuroimage 58 (3) (2011) 732–740.
[43] K. Hikishima, et al., In vivo microscopic voxel-based morphometry with a brain template to characterize strain-specific structures in the mouse brain, Sci. Rep. 7 (1) (2017) 85.
[44] B.R. Sajja, et al., Generation and disease model relevance of a manganese enhanced magnetic resonance imaging-based NOD/scid-IL-2Rgammac(null) mouse brain atlas, J. Neuroimmune Pharmacol. 11 (1) (2016) 133–141.
[45] S.J. Sawiak, N.I. Wood, G.B. Williams, A.J. Morton, T.A. Carpenter, Voxel-based morphometry with templates and validation in a mouse model of Huntington's disease, Magn. Reson. Imaging 31 (9) (2013) 1522–1531.
[46] S.J. Sawiak, N.I. Wood, G. Williams, A. Morton, T. Carpenter Spmmouse, A new toolbox for SPM in the animal brain, in: ISMRM 17th Scientific Meeting & Exhibition, April. 2009.
[47] N. Chuang, et al., An MRI-based atlas and database of the developing mouse brain, Neuroimage 54 (1) (2011) 80–89.
[48] Y. Jiang, G.A. Johnson, Microscopic diffusion tensor atlas of the mouse brain, Neuroimage 56 (3) (2011) 1235–1243.
[49] M. Hawrylycz, et al., Digital atlasing and standardization in the mouse brain, PLoS Comput. Biol. 7 (2) (2011) e1001065.
[50] A.A. Sharief, A. Badea, A.M. Dale, G.A. Johnson, Automated segmentation of the actively stained mouse brain using multi-spectral MR microscopy, Neuroimage 39 (1) (2008) 136–145.
[51] A. Badea, A.A. Ali-Sharief, G.A. Johnson, Morphometric analysis of the C57BL/6J mouse brain, Neuroimage 37 (3) (2007) 683–693.
[52] A.A. Ali, A.M. Dale, A. Badea, G.A. Johnson, Automated segmentation of neuroanatomical structures in multispectral MR microscopy of the mouse brain, Neuroimage 27 (2) (2005) 425–435.
[53] H. Benveniste, K. Kim, L. Zhang, G.A. Johnson, Magnetic resonance microscopy of the C57BL mouse brain, Neuroimage 11 (6 Pt 1) (2000) 601–611.
[54] Y. Ma, et al., *In* vivo 3D digital atlas database of the adult C57bl/6J mouse brain by magnetic resonance microscopy, Front. Neuroanat. 2 (2008) 1.
[55] Y. Ma, et al., A three-dimensional digital atlas database of the adult C57BL/6J mouse brain by magnetic resonance microscopy, Neuroscience 135 (4) (2005) 1203–1215.
[56] A.E. Dorr, J.P. Lerch, S. Spring, N. Kabani, R.M. Henkelman, High resolution three-dimensional brain atlas using an average magnetic resonance image of 40 adult C57Bl/6J mice, Neuroimage 42 (1) (2008) 60–69.
[57] A. Dorr, J.G. Sled, N. Kabani, Three-dimensional cerebral vasculature of the CBA mouse brain: a magnetic resonance imaging and micro computed tomography study, Neuroimage 35 (4) (2007) 1409–1423.
[58] X.J. Chen, et al., Neuroanatomical differences between mouse strains as shown by high-resolution 3D MRI, Neuroimage 29 (1) (2006) 99–105.
[59] N. Kovacevic, et al., A three-dimensional MRI atlas of the mouse brain with estimates of the average and variability, Cerebr. Cortex 15 (5) (2005) 639–645.
[60] A.J. Mackenzie-Graham, et al., Multimodal, multidimensional models of mouse brain, Epilepsia 48 (Suppl 4) (2007) 75–81. Suppl 4.
[61] N.A. Bock, et al., In vivo magnetic resonance imaging and semiautomated image analysis extend the brain phenotype for cdf/cdf mice, J. Neurosci. 26 (17) (2006) 4455–4459.

[62] E.F. Lee, R.E. Jacobs, I. Dinov, A. Leow, A.W. Toga, Standard atlas space for C57BL/6J neonatal mouse brain, Anat. Embryol. 210 (4) (2005) 245–263.
[63] Y. Yang, et al., In vivo symmetric multi-contrast MRI brain templates and atlas for spontaneously hypertensive rats, Brain Struct. Funct. 227 (5) (2022) 1789–1801.
[64] G.A. Johnson, et al., A multicontrast MR atlas of the Wistar rat brain, Neuroimage 242 (2021) 118470.
[65] E. Calabrese, A. Badea, C. Watson, G.A. Johnson, A quantitative magnetic resonance histology atlas of postnatal rat brain development with regional estimates of growth and variability, Neuroimage 71 (2013) 196–206.
[66] G.A. Johnson, E. Calabrese, A. Badea, G. Paxinos, C. Watson, A multidimensional magnetic resonance histology atlas of the Wistar rat brain, Neuroimage 62 (3) (2012) 1848–1856.
[67] G.A. Johnson, M.B. Thompson, B.P. Drayer, Three-dimensional MRI microscopy of the normal rat brain, Magn. Reson. Med. 4 (4) (1987) 351–365.
[68] M.J.W. Prior, et al., Ratlas-LH: an MRI template of the Lister hooded rat brain with stereotaxic coordinates for neurosurgical implantations, Brain Neurosci. Adv. 5 (2021) 23982128211036332.
[69] D. Goerzen, et al., An MRI-derived neuroanatomical atlas of the fischer 344 rat brain, Sci. Rep. 10 (1) (2020) 6952.
[70] D.A. Barriere, et al., The SIGMA rat brain templates and atlases for multimodal MRI data analysis and visualization, Nat. Commun. 10 (1) (2019) 5699.
[71] K. Wisner, B. Odintsov, D. Brozoski, T.J. Brozoski, Ratat1: a digital rat brain stereotaxic atlas derived from high-resolution MRI images scanned in three dimensions, Front. Syst. Neurosci. 10 (2016) 64.
[72] M. Figini, et al., In vivo DTI tractography of the rat brain: an atlas of the main tracts in Paxinos space with histological comparison, Magn. Reson. Imaging 33 (3) (2015) 296–303.
[73] S. Lancelot, et al., A multi-atlas based method for automated anatomical rat brain MRI segmentation and extraction of PET activity, PLoS One 9 (10) (2014) e109113.
[74] A. Rumple, et al., 3-dimensional diffusion tensor imaging (DTI) atlas of the rat brain, PLoS One 8 (7) (2013) e67334.
[75] B. Nie, et al., A rat brain MRI template with digital stereotaxic atlas of fine anatomical delineations in paxinos space and its automated application in voxel-wise analysis, Hum. Brain Mapp. 34 (6) (2013) 1306–1318.
[76] P.A. Valdes-Hernandez, et al., An in vivo MRI template set for morphometry, tissue segmentation, and fMRI localization in rats, Front. Neuroinf. 5 (2011) 26.
[77] J. Veraart, et al., Population-averaged diffusion tensor imaging atlas of the Sprague Dawley rat brain, Neuroimage 58 (4) (2011) 975–983.
[78] K.R. Thomas, M.R. Capecchi, Site-directed mutagenesis by gene targeting in mouse embryo-derived stem cells, Cell 51 (3) (1987) 503–512.
[79] T.J. Aitman, et al., Progress and prospects in rat genetics: a community view, Nat. Genet. 40 (5) (2008) 516–522.
[80] C. Tong, G. Huang, C. Ashton, P. Li, Q.L. Ying, Generating gene knockout rats by homologous recombination in embryonic stem cells, Nat. Protoc. 6 (6) (2011) 827–844.
[81] Y. Shao, et al., CRISPR/Cas-mediated genome editing in the rat via direct injection of one-cell embryos, Nat. Protoc. 9 (10) (2014) 2493–2512.
[82] R.A. Gibbs, et al., Genome sequence of the Brown Norway rat yields insights into mammalian evolution, Nature 428 (6982) (2004) 493–521.
[83] M. Shimoyama, et al., Exploring human disease using the rat genome database, Dis. Model Mech. 9 (10) (2016) 1089–1095.
[84] C. Francis, et al., Divergence of RNA localization between rat and mouse neurons reveals the potential for rapid brain evolution, BMC Genom. 15 (2014) 883.
[85] Y. Ren, A.A. Palmer, Behavioral genetic studies in rats, Methods Mol. Biol. 2018 (2019) 319–326.
[86] J.P. Munasinghe, G.A. Gresham, T.A. Carpenter, L.D. Hall, Magnetic resonance imaging of the normal mouse brain: comparison with histologic sections, Lab. Anim. Sci. 45 (6) (1995) 674–679.
[87] M. Brackhan, et al., [(18) F]GE180 positron emission tomographic imaging indicates a potential double-hit insult in the intrahippocampal kainate mouse model of temporal lobe epilepsy, Epilepsia 59 (3) (2018) 617–626.
[88] T.W. Uselman, D.R. Barto, R.E. Jacobs, E.L. Bearer, Evolution of brain-wide activity in the awake behaving mouse after acute fear by longitudinal manganese-enhanced MRI, Neuroimage 222 (2020) 116975.
[89] A. Badea, G.A. Johnson, R.W. Williams, Genetic dissection of the mouse CNS using magnetic resonance microscopy, Curr. Opin. Neurol. 22 (4) (2009) 379–386.
[90] C.E.M. Golden, V.X. Wang, H. Harony-Nicolas, P.R. Hof, J.D. Buxbaum, Reduced brain volume and white matter alterations in Shank3-deficient rats, Autism Res. 14 (9) (2021) 1837–1842.
[91] E. Lüders, H. Steinmetz, L. Jäncke, Brain size and grey matter volume in the healthy human brain, Neuroreport 13 (17) (2002) 2371–2374.
[92] G.A. Johnson, et al., High-throughput morphologic phenotyping of the mouse brain with magnetic resonance histology, Neuroimage 37 (1) (2007) 82–89.
[93] P.J. Basser, C. Pierpaoli, Microstructural and physiological features of tissues elucidated by quantitative-diffusion-tensor MRI, J. Magn. Reson. B 111 (3) (1996) 209–219.
[94] C. Beaulieu, The basis of anisotropic water diffusion in the nervous system - a technical review, NMR Biomed. 15 (7–8) (2002) 435–455.
[95] R.X. Moldrich, et al., Comparative mouse brain tractography of diffusion magnetic resonance imaging, Neuroimage 51 (3) (2010) 1027–1036.
[96] S. Mori, P.C. van Zijl, Fiber tracking: principles and strategies - a technical review, NMR Biomed. 15 (7–8) (2002) 468–480.
[97] S. Mori, et al., Diffusion tensor imaging of the developing mouse brain, Magn. Reson. Med. 46 (1) (2001) 18–23.
[98] J. Zhang, et al., Three-dimensional anatomical characterization of the developing mouse brain by diffusion tensor microimaging, Neuroimage 20 (3) (2003) 1639–1648.
[99] J. Lee, et al., Evaluation of atlas based mouse brain segmentation, Proc. SPIE-Int. Soc. Opt. Eng. 7259 (2009) 725943–725949.
[100] B. Nie, et al., Automatic method for tracing regions of interest in rat brain magnetic resonance imaging studies, J. Magn. Reson. Imag. 32 (4) (2010) 830–835.
[101] I. Oguz, et al., Comparison of magnetic resonance imaging in live vs. post mortem rat brains, PLoS One 8 (8) (2013) e71027.
[102] M. Goubran, et al., Multimodal image registration and connectivity analysis for integration of connectomic data from microscopy to MRI, Nat. Commun. 10 (1) (2019) 5504.
[103] A. Boitnott, et al., Developmental and behavioral phenotypes in a mouse model of DDX3X syndrome, Biol. Psychiatr. 90 (11) (2021) 742–755.
[104] M. Ingalhalikar, et al., Connectome and maturation profiles of the developing mouse brain using diffusion tensor imaging, Cerebr. Cortex 25 (9) (2015) 2696–2706.
[105] V. Zerbi, et al., Rapid reconfiguration of the functional connectome after chemogenetic locus coeruleus activation, Neuron 103 (4) (2019) 702–718 e5.
[106] G. Del Ferraro, et al., Finding influential nodes for integration in brain networks using optimal percolation theory, Nat. Commun. 9 (1) (2018) 2274.
[107] C.A. Gharagouzloo, et al., Quantitative vascular neuroimaging of the rat brain using superparamagnetic nanoparticles: new insights on vascular organization and brain function, Neuroimage 163 (2017) 24–33.
[108] M. Brendel, et al., Late-stage Anle138b treatment ameliorates tau pathology and metabolic decline in a mouse model of human Alzheimer's disease tau, Alzheimer's Res. Ther. 11 (1) (2019) 67.
[109] C. Nicolas, et al., Longitudinal changes in brain metabolic activity after withdrawal from escalation of cocaine self-administration, Neuropsychopharmacology 42 (10) (2017) 1981–1990.
[110] T. Blume, et al., Microglial response to increasing amyloid load saturates with aging: a longitudinal dual tracer in vivo muPET-study, J. Neuroinflammation 15 (1) (2018) 307.
[111] M. Maruyama, et al., Imaging of tau pathology in a tauopathy mouse model and in Alzheimer patients compared to normal controls, Neuron 79 (6) (2013) 1094–1108.
[112] R. Li, et al., Mapping accumulative whole-brain activities during environmental enrichment with manganese-enhanced magnetic resonance imaging, Neuroimage 210 (2020) 116588.
[113] J. Grandjean, et al., A brain-wide functional map of the serotonergic responses to acute stress and fluoxetine, Nat. Commun. 10 (1) (2019) 350.
[114] G. Bar-Klein, et al., Imaging blood-brain barrier dysfunction as a biomarker for epileptogenesis, Brain 140 (6) (2017) 1692–1705.
[115] V. Beaumont, et al., Phosphodiesterase 10A inhibition improves cortico-basal ganglia function in huntington's disease models, Neuron 92 (6) (2016) 1220–1237.

[116] M. Michaelides, et al., Whole-brain circuit dissection in free-moving animals reveals cell-specific mesocorticolimbic networks, J. Clin. Invest. 123 (12) (2013) 5342–5350.
[117] E. Chan, N. Kovacevic, S.K. Ho, R.M. Henkelman, J.T. Henderson, Development of a high resolution three-dimensional surgical atlas of the murine head for strains 129S1/SvImJ and C57Bl/6J using magnetic resonance imaging and micro-computed tomography, Neuroscience 144 (2) (2007) 604–615.
[118] A. De Barros, G. Arribarat, J. Combis, P. Chaynes, P. Peran, Matching ex vivo MRI with iron histology: pearls and pitfalls, Front. Neuroanat. 13 (2019) 68.
[119] A.E. de Guzman, M.D. Wong, J.A. Gleave, B.J. Nieman, Variations in post-perfusion immersion fixation and storage alter MRI measurements of mouse brain morphometry, Neuroimage 142 (2016) 687–695.
[120] H.F. Wehrl, et al., Assessment of murine brain tissue shrinkage caused by different histological fixatives using magnetic resonance and computed tomography imaging, Histol. Histopathol. 30 (5) (2015) 601–613.
[121] H. Kleven, et al., AtOM, an ontology model to standardize use of brain atlases in tools, workflows, and data infrastructures, Sci. Data 10 (1) (2023) 486.